



Tool from ancient pharmacopoeia prevents vision loss

[Jeffrey Boatright](#), *Emory University*

Anisha G. Moring, *affiliation*

Clinton McElroy, *affiliation*

Michael J. Phillips, *affiliation*

Vi T. Do, *affiliation*

Bo Chang, *affiliation*

Norm L. Hawes, *affiliation*

Amber P. Boyd, *affiliation*

Sheree S. Sidney, *affiliation*

Rachael E. Stewart, *affiliation*

Only first 10 authors above; see publication for full author list.

Journal Title: Molecular Vision

Volume: Volume 2006, Number 12

Publisher: Molecular Vision | 2006-12-29, Pages 1706-1714

Type of Work: Article | Final Publisher PDF

Permanent URL: <http://pid.emory.edu/ark:/25593/f8n3c>

Final published version: <http://www.molvis.org/molvis/v12/a195/>

Copyright information:

©2006 Molecular Vision

This is an Open Access article distributed under the terms of the Creative Commons Attribution-NonCommercial-NoDerivs 3.0 Unported License (<http://creativecommons.org/licenses/by-nc-nd/3.0/>), which permits making multiple copies, distribution, public display, and publicly performance, provided the original work is properly cited. This license requires copyright and license notices be kept intact, credit be given to copyright holder and/or author. This license prohibits exercising rights for commercial purposes.



Accessed August 22, 2022 10:09 AM EDT



Tool from ancient pharmacopoeia prevents vision loss

Jeffrey H. Boatright,¹ Anisha G. Moring,¹ Clinton McElroy,^{1,2} Michael J. Phillips,^{1,2} Vi T. Do,¹ Bo Chang,³ Norm L. Hawes,³ Amber P. Boyd,¹ Sheree S. Sidney,¹ Rachael E. Stewart,¹ Steven C. Minear,¹ Rajashree Chaudhury,¹ Vincent T. Ciavatta,^{1,2} Cecilia M.P. Rodrigues,⁴ Clifford J. Steer,⁵ John M. Nickerson,¹ Mabelle T. Pardue^{1,2}

¹Department of Ophthalmology, Emory University School of Medicine, Atlanta, GA; ²Atlanta VA Medical Center, Research Service, Decatur, GA; ³The Jackson Laboratory, Bar Harbor, ME; ⁴Centro de Patogenese Molecular, Faculty of Pharmacy, University of Lisbon, Lisbon, Portugal; ⁵Department of Medicine, University of Minnesota Medical School, Minneapolis, MN

Purpose: Bear bile has been used in Asia for over 3,000 years to treat visual disorders, yet its therapeutic potential remains unexplored in Western vision research. The purpose of this study was to test whether treatment of mice undergoing retinal degeneration with tauroursodeoxycholic acid (TUDCA), a primary constituent of bear bile, alters the course of degeneration.

Methods: Two retinal degeneration models were tested: the *rd10* mouse, which has a point mutation in the gene encoding the beta subunit of rod phosphodiesterase, and light induced retinal damage (LIRD). For LIRD studies, albino Balb/C adult mice were subcutaneously injected with TUDCA (500 mg/kg body weight) or vehicle (0.15 M NaHCO₃). Sixteen h later, each mouse received repeat injections. Half of each treatment group was then placed in bright light (10,000 lux) or dim light (200 lux) for seven h. At the end of exposure, animals were transferred to their regular housing. Electroretinograms (ERGs) were assessed 24 h later, mice sacrificed, eyes embedded in paraffin and sectioned, and retina sections assayed for morphology and apoptosis by TUNEL and anti-active caspase-3 immunoreactivity via fluorescent confocal microscopy. A subset of mice were sacrificed 8 and 15 days after exposure and retina sections analyzed for morphology and apoptosis. For *rd10* studies, mice were injected subcutaneously with TUDCA or vehicle at postnatal (P) days 6, 9, 12, and 15. At p18, ERGs were recorded, mice were euthanized and eyes were harvested, fixed, and processed. Retinal sections were stained (toluidine blue), and retinal cell layers morphometrically analyzed by light microscopy. Consecutive sections were analyzed for apoptosis as above.

Results: By every measure, TUDCA greatly slowed retinal degeneration in LIRD and *rd10* mice. ERG a-wave and b-wave amplitudes were greater in mice treated with TUDCA compared to those treated with vehicle. Retinas of TUDCA-treated mice had thicker outer nuclear layers, more photoreceptor cells, and more fully-developed photoreceptor outer segments. Finally, TUDCA treatments dramatically suppressed signs of apoptosis in both models.

Conclusions: Systemic injection of TUDCA, a primary constituent of bear bile, profoundly suppressed apoptosis and preserved function and morphology of photoreceptor cells in two disparate mouse models of retinal degeneration. It may be that bear bile has endured so long in Asian pharmacopoeias due to efficacy resulting from this anti-apoptotic and neuroprotective activity of TUDCA. These results also indicate that a systematic, clinical assessment of TUDCA may be warranted.

Ancient and modern Asian pharmacopoeias classify bear bile as a bitter, “cold” medicine used for detoxifying the liver, dissolving kidney stones and gallstones, relieving convulsions, and improving vision [1,2]. Notably, of the 28 types of Chinese patent medicines containing bear bile, 15 are ophthalmologic [2]. While bear bile has been used in Asia for over 3,000 years to treat visual disorders [1,2], its therapeutic potential remains unexplored in Western vision research. Might the ancient and modern vision-rescue claims made about bear bile be tested in animal models of human retinal degeneration?

To answer this question, we assessed the effect of systemic injection of tauroursodeoxycholic acid (TUDCA), a primary constituent of bear bile [1,3], in two animal models of retinal degeneration, the *Pde6b^{rd10}* (*rd10*) mouse, a genetic

model of blindness [4,5], and the light-induced retinal degeneration (LIRD) mouse, an environmental model of blindness [6,7]. Mouse strains that have mutations in the β subunit of rod photoreceptor cGMP phosphodiesterase (such as *rd10*) and LIRD rodent protocols are some of the oldest and most-studied models of retinal disease [4,6].

Here we show that systemic injection of synthetic TUDCA prevented apoptosis and preserved function and morphology of photoreceptor cells in hereditary and environmental mouse models of human retinal degeneration. The results suggest an efficacy for this component of an ancient ophthalmic pharmaceutical.

METHODS

Animals: All animal procedures were approved by the Institutional Animal Care and Use Committee and conform to the standards of the Association for Research in Vision and Ophthalmology. C57/B16J, BALB/C, and *rd10* mice were obtained from Jackson Laboratories (Bar Harbor, ME) and were bred

Correspondence to: Jeffrey H. Boatright, Ph.D., Associate Professor, Department of Ophthalmology, Emory University, B55511, 1365B Clifton Road, N.E., Atlanta, GA, 30322; Phone: (404) 778-4113; FAX: (404) 778-2231; email: jboatr@emory.edu

and raised under 12:12 light:dark cycle and fed ad libitum standard Purina mouse chow.

For LIRD experiments, adult BALB/C mice were weighed and injected subcutaneously in the nape of the neck with either vehicle (0.15 M NaHCO₃, 1 ml/kg) or vehicle containing TUDCA (500 mg/kg; Calbiochem, La Jolla, CA) [8], dark-adapted for 18 h, injected again, then exposed to 7 h of bright (10,000 lux) or dim (200 lux) light [7]. TUDCA and vehicle solutions were made fresh prior to every injection and pH adjusted to 7.4. Visual function was assessed by electroretinography (ERG) 24 h later, after which mice were sacrificed and eyes prepared for morphological and biochemical analyses. A subset of animals was sacrificed two weeks later and retinas prepared for additional morphological and biochemical analyses.

For hereditary model experiments, *rd10* mice were weighed and injected with vehicle or TUDCA (formulation as above) at postnatal (P) days 6, 9, 12, and 15. At P18, a stage by which photoreceptor degeneration and visual function loss are pronounced in *rd10* mice [4,5], ERGs were recorded, mice sacrificed, and eyes prepared for morphological and biochemical analyses.

Bile acid analysis of brain tissue: Brains were removed, flash frozen and stored at -70 °C. Bile acids were assessed by gas chromatography after organic solvent extraction, purification on Lipidex 1000, liquid-solid extraction, hydrolysis, isolation by lipophilic anion exchange chromatography and conversion to methyl ester-trimethylsilyl ether derivatives [9]. Bile acid concentrations were expressed as nmol/g of tissue.

Electroretinogram (ERG) methods: ERGs were recorded on mice dark-adapted overnight using a UTAS-E3000 recording system (LKC, Gaithersburg, MD) as previously detailed [5,10-12]. Briefly, anesthetized mice (ketamine 80 mg/kg and xylazine 16/mg/kg) were placed on a heating pad inside a Faraday cage in front of a desktop Ganzfeld. The active electrode was a silver wire loop on the cornea, the reference electrode was a 1-cm platinum needle placed in the cheek, and the ground electrode was a needle placed in the tail. For *rd10* mice, dark-adapted ERG responses to a series of increasing-intensity light flashes ranging from 0.00039 to 137 cd sec/m² were averaged over 5 to 10 separate flashes per light intensity. The inter-stimulus time was increased from 10 to 60 s as flash intensities were increased. LIRD mice were tested with only the brightest flash intensity, 137 cd sec/m².

To measure ERG amplitude, the a-wave was measured from the baseline to the trough of the first negative wave. The b-wave was measured from the trough of the a-wave to the peak of the first positive wave, or when the a-wave was not present, from baseline to the peak of the first positive wave.

Histology and morphometrics: Morphological assessment of retinal sections was done essentially as previously detailed [5,10-12]. Following ERG recordings, eyes were marked on the superior portion of the limbus using a permanent marker while still in the eye socket for orientation. Eyes were enucleated, immersion-fixed in 4% paraformaldehyde for 30 min, and then stored in phosphate-buffered saline for later histological or apoptosis analysis. For histological analysis, eyes

were dehydrated through a graded alcohol series and embedded in Embed 812/DER 736 plastic medium (Electron Microscopy Science, Inc, Hatfield, PA). Sections (0.5 μm) bisecting the optic disc superiorly to inferiorly were cut on an Reichert Ultracut ultramicrotome (Leica Inc., Deerfield, IL) using a histo-diamond knife and heat fixed to glass slides. Staining was done with 1% aqueous toluidine blue (Sigma; St. Louis, MO).

For each section, two 400 μm-wide areas, one approximately 150 μm superior to the optic disc and one approximately 150 μm inferior to the optic disc, were acquired as Adobe Photoshop images at 200X magnification. Photoreceptor nuclei counts and thickness measurements for the outer nuclear layer and photoreceptor outer segments were made using Image Tool (UTHSCSA, San Antonio, TX). For each image, 5 locations were measured and those values averaged together as the representative measurements for that section. Five sections were averaged for each eye. Student's t-tests were used to compare means of vehicle versus TUDCA treated groups.

Apoptosis measurements via TUNEL and activated caspase-3: Fluorescent TUNEL signal in retinal sections was used as a measure of apoptosis as previously described [5]. Briefly, microtome-cut paraffin sections (5 μm) bisecting the optic disc superiorly to inferiorly were stained by terminal deoxynucleotidyl transferase-mediated 2'-deoxyuridine 5'-triphosphate-biotin nick end labeling (TUNEL) using a DeadEnd Fluorometric TUNEL kit (Promega, Madison, WI) and counter-stained with propidium iodide. Images of sections were captured by computer-aided confocal microscopy and photoreceptor nuclei counted per field as above. For each field, percentages of apoptotic-to-total nuclei were averaged across three or more observers and those means averaged within treatment group. Student's t-tests were used to compare the means of vehicle versus TUDCA treated groups.

Apoptosis was also assessed by immunohistochemical staining of retina sections with an antibody specific for activated caspase-3 following manufacturer instructions (Promega). Briefly, paraffin-embedded retina sections were deparaffinized in xylene, permeabilized in Triton X-100, then incubated with anti-active caspase-3 primary antibody followed by donkey anti-rabbit Cy3 (MTP2) conjugated secondary antibody, and counter-stained with propidium iodide. Sections were examined with the confocal microscope, as described with the TUNEL labeling. Additionally, for some samples fluorescence was obtained across entire retina sections by using the magic wand function of Photoshop to select the ONL, then using the luminosity function to measure mean pixel luminosity. This was used as another method to quantify the fluorescence resulting from TUNEL or from activated caspase-3 immunoreactivity.

RESULTS

Effect of subcutaneous TUDCA injections on brain levels of TUDCA: The accumulation of TUDCA in the brains of injected mice was measured to determine whether injections alter neuronal tissue levels of TUDCA. Retina tissue levels of

TUDCA and other bile acids were too low to measure with current technologies (data not shown). Subcutaneous injections of TUDCA at P6, 9, and 15 elevated whole brain levels of TUDCA in P18 mice (0.61 ± 0.06 nmol/g TUDCA-injected versus 0.06 ± 0.01 nmol/g vehicle-injected; $n=6$ per treatment; $p < 0.0001$).

Effect of TUDCA treatment on LIRD mice: Bright light exposure caused massive disruption of photoreceptor cells and extreme disorganization of the outer nuclear layer (ONL) at durations as short as 24 h post-exposure in vehicle-treated mice (Figure 1). Conversely, retinas from TUDCA-treated mice showed few morphological effects of bright light exposure. Of note is the extent of damage to cells in the ONL; nearly the entire ONL of vehicle-treated mice had damage, whereas in TUDCA-treated mice almost no morphological damage was observed across the ONL (Figure 1). By 15 days post-exposure to bright light, the damage caused by light exposure, and prevention thereof by TUDCA treatment, was even more dra-

matic (Figure 2). TUDCA treatment preserved the normal vertical stacking of the photoreceptor nuclei while the nuclei in the vehicle-treated eyes appear in extreme disarray (Figure 2). ONL thickness was greatly reduced in vehicle-treated mice versus TUDCA-treated mice (means \pm SEM: 15.0 ± 3.75 versus 42.6 ± 2.61 μ m, respectively; $p=0.0034$, $t=4.343$, $df=7$; Figure 2). Exposure to dim light did not cause significant cell death as noted by cell counts and general retinal morphology.

Bright light exposure drastically suppressed ERG a-wave and b-wave amplitudes in vehicle-treated mice compared to dim light exposure (Figure 3 and Figure 4). TUDCA treatment had no effect on mice exposed to dim light, but it largely prevented loss of function in mice exposed to bright light (Figure 3 and Figure 4). Dark-adapted ERG a- and b-wave amplitudes were significantly greater for TUDCA- versus vehicle-treated mice following bright light exposure, and indeed, were not statistically different from responses from mice exposed to dim light (Figure 4; the statistical analysis was simple

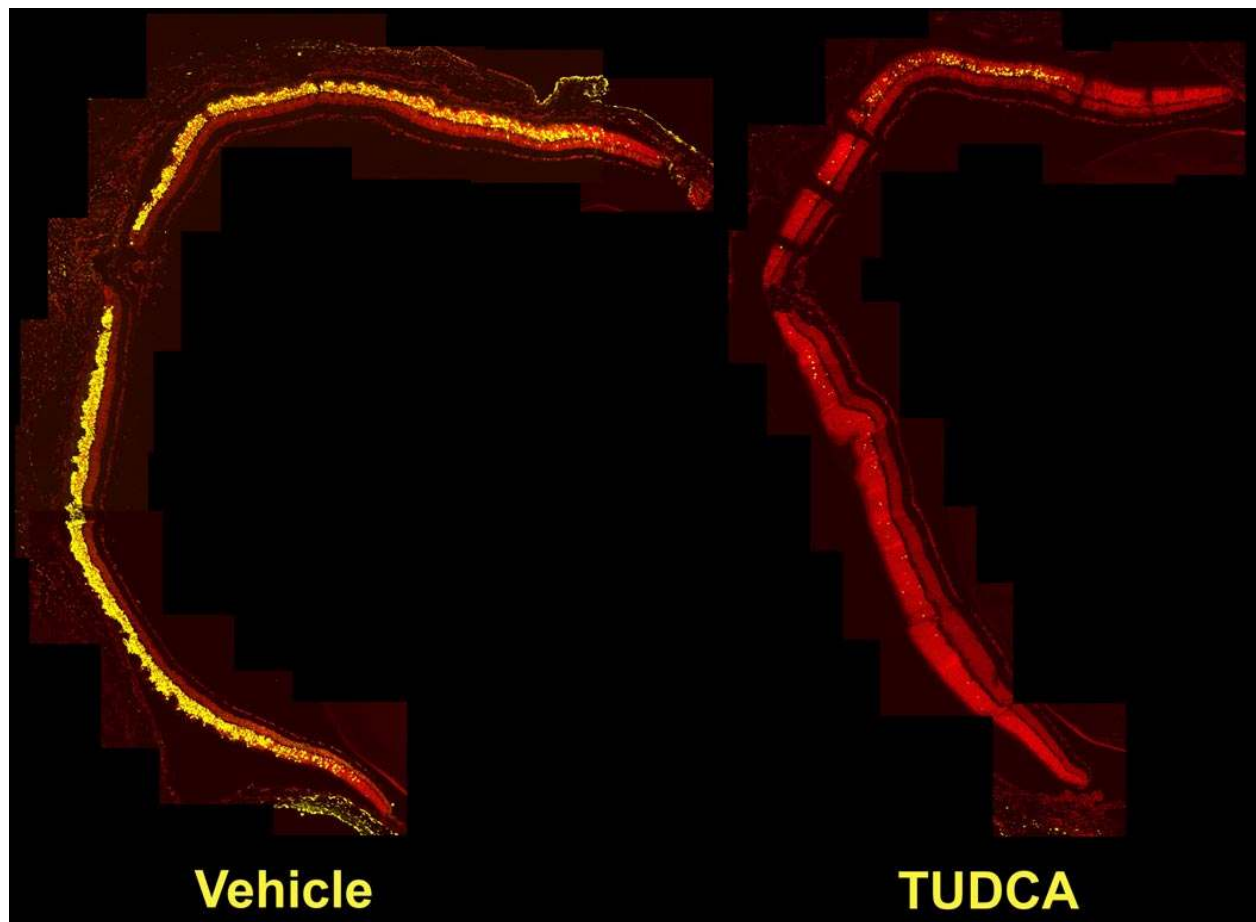


Figure 1. Effect of TUDCA on LIRD mouse retina morphology and apoptosis: 24 h post-light exposure. Composite images of confocal micrographs of LIRD mouse retina sections assayed for apoptosis by fluorescent TUNEL. The images were assembled into a composite from confocal micrographs laid over one another in Photoshop to provide a complete image of a retina section. A representative composite of the results obtained with vehicle (left) versus TUDCA (right) injections is shown. In each composite, the optic nerve is to the left and the cornea, which was removed, would be to the right. The composites represent the full diameter of the adult eye, which is approximately 3 mm. Bright light exposure induced massive apoptosis (yellow signal) and morphological damage in photoreceptor cells and retinal outer nuclear layer of vehicle-treated (left) but not TUDCA-treated eyes (right). The percentage of TUNEL-positive photoreceptors was greatly reduced in TUDCA- versus vehicle-treated LIRD mice ($49.4 \pm 11\%$ versus $11.9 \pm 4.2\%$; $p=0.0074$, $t=3.443$, $df=9$; counts per field as detailed in Methods).

ANOVA with Newman-Keuls post-hoc analysis, the asterisk indicates a $p < 0.005$).

TUDCA injections suppressed apoptosis in LIRD mice. Bright light exposure resulted in wide-spread apoptosis in the ONL (but not other nuclear layers) of retinas from vehicle-treated mice as assessed by TUNEL (Figure 1 and Figure 2). Conversely, TUNEL signal was nearly absent in ONL of TUDCA-treated mice (Figure 1 and Figure 2). The percent-

age of TUNEL-positive photoreceptors was greatly reduced in TUDCA- versus vehicle-treated mice exposed to bright light ($11.9 \pm 4.2\%$ versus $49.4 \pm 11\%$; $p = 0.0074$, $t = 3.443$, $df = 9$). Similarly, immunoreactivity for activated caspase-3 was virtually nonexistent in sections from TUDCA-injected mice yet abundant in retina sections from vehicle-injected mice (mean pixel luminosity per whole retina section: 0.26 ± 0.05 versus 3.12 ± 0.36 ; $n = 24/\text{group}$; $p = 0.0001$ by Student's *t*-test; Figure

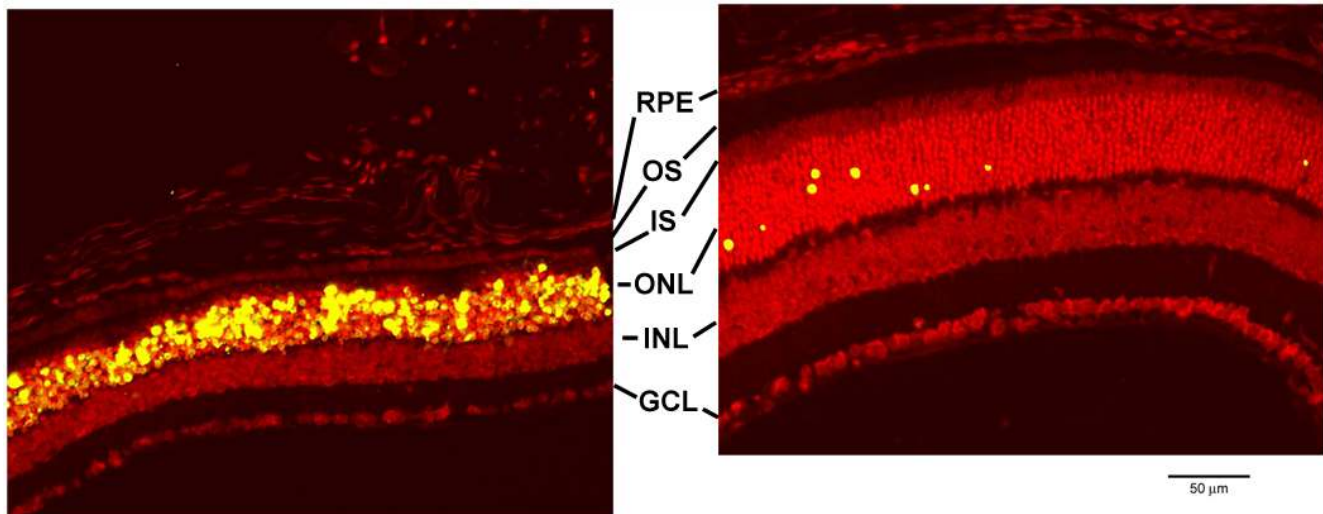


Figure 2. Effect of TUDCA on LIRD mouse retina morphology and apoptosis: 15 days post-light exposure. Confocal micrographs of LIRD mouse retina sections assayed for apoptosis by fluorescent TUNEL. Bright light exposure induced massive apoptosis and morphological damage in retinal photoreceptors of vehicle-treated (left) but not TUDCA-treated eyes (right). Of particular note in the vehicle-treated sample is the thinning of the outer nuclear layer (ONL) and the nearly-complete loss of inner segments (IS) and outer segments (OS) of the photoreceptors. Additionally, nearly all the photoreceptor nuclei are TUNEL-positive. Conversely, TUDCA-treated samples showed intact photoreceptors, thick ONL, and very few TUNEL-positive photoreceptor cells. Treatment had no discernable effect on the inner nuclear layer (INL), ganglion cell layer (GCL), or retinal pigment epithelium (RPE).

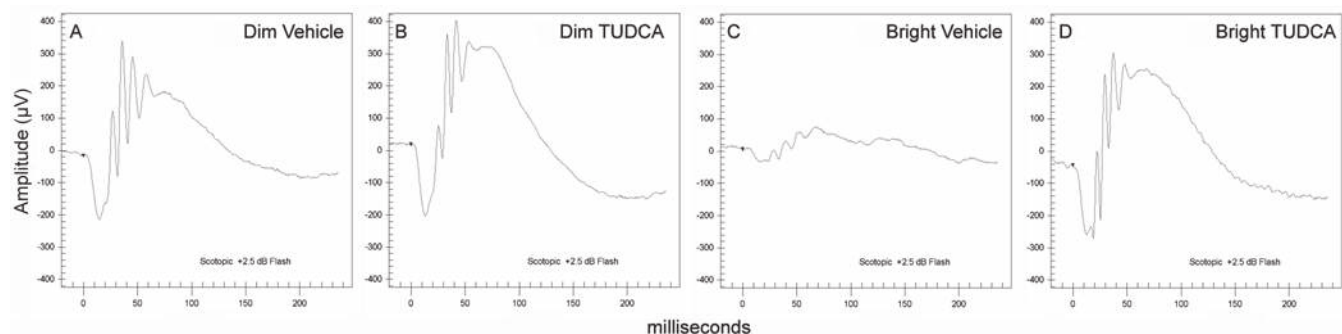


Figure 3. Effect of TUDCA on LIRD mouse retina function: Representative ERG traces at 24 h post-light exposure. To test whether TUDCA protects the retina from bright-light damage, mice were pretreated with TUDCA or vehicle only and then exposed to bright or dim light. After light treatment (24 h), electroretinograms (ERGs) were recorded as an outcome measure of retina function. Representative ERGs are shown, in response to a 137 cd sec/m² Ganzfeld flash (+2.5 dB). **A** illustrates a mouse that received vehicle only and was exposed to dim light. This represents a normal ERG profile for this ERG flash stimulus. **B** is from a mouse treated with TUDCA and exposed to dim light. This tracing is normal, suggesting that TUDCA by itself does not affect the ERG. **C** was recorded from a mouse that was treated with vehicle only and exposed to bright light. This condition reflects extensive damage to the retina, and the ERG shows a greatly diminished a-wave, b-wave, and oscillatory potentials. **D** illustrates a trace recorded from a mouse treated with TUDCA and exposed to bright light. The ERG is very similar to the response shown in **A**, the vehicle treated dim-light mouse, suggesting that retina function is unimpaired. The implicit times are the same among all four groups, and the number of oscillatory potential peaks appears the same. This experiment shows that major differences are the profound loss of ERG signal (about 80% reduction) following light damage, and the apparent full protection from light damage by TUDCA.

5). Exposure to dim light did not cause significant cell death as noted by cell counts, TUNEL or caspase-3 labeling.

Effect of TUDCA on rd10 mice: The data from the LIRD experiments demonstrate that TUDCA can prevent retinal degeneration when treatment precedes an environmental insult. Of additional importance to the clinical setting is testing whether TUDCA treatment alters retinal degeneration in a genetic model. Accordingly, *rd10* mice were injected with vehicle or TUDCA from P6 through P15. At P18, a stage by which photoreceptor degeneration and visual function loss are pronounced in *rd10* mice [4,5], ERGs were recorded and morphological and biochemical analyses of the retina were performed.

TUDCA injections preserved retinal photoreceptor cell function in rd10 mice: TUDCA treatment resulted in significantly greater dark-adapted ERG a- and b-wave amplitudes compared to vehicle treatment, indicating preservation of retinal function (Figure 6; Repeated measures ANOVA:

Figure 4. Effect of TUDCA on LIRD mouse retina function: Quantification at 24 h post-light exposure. Bright light exposure suppressed ERG a-wave and b-wave amplitudes to a bright Ganzfeld flash (137 cd sec/m²); TUDCA treatment completely prevented this loss of function (simple ANOVA with Newman-Keuls post-hoc analysis, N=7-9/per group, The asterisk indicates a p<0.005).

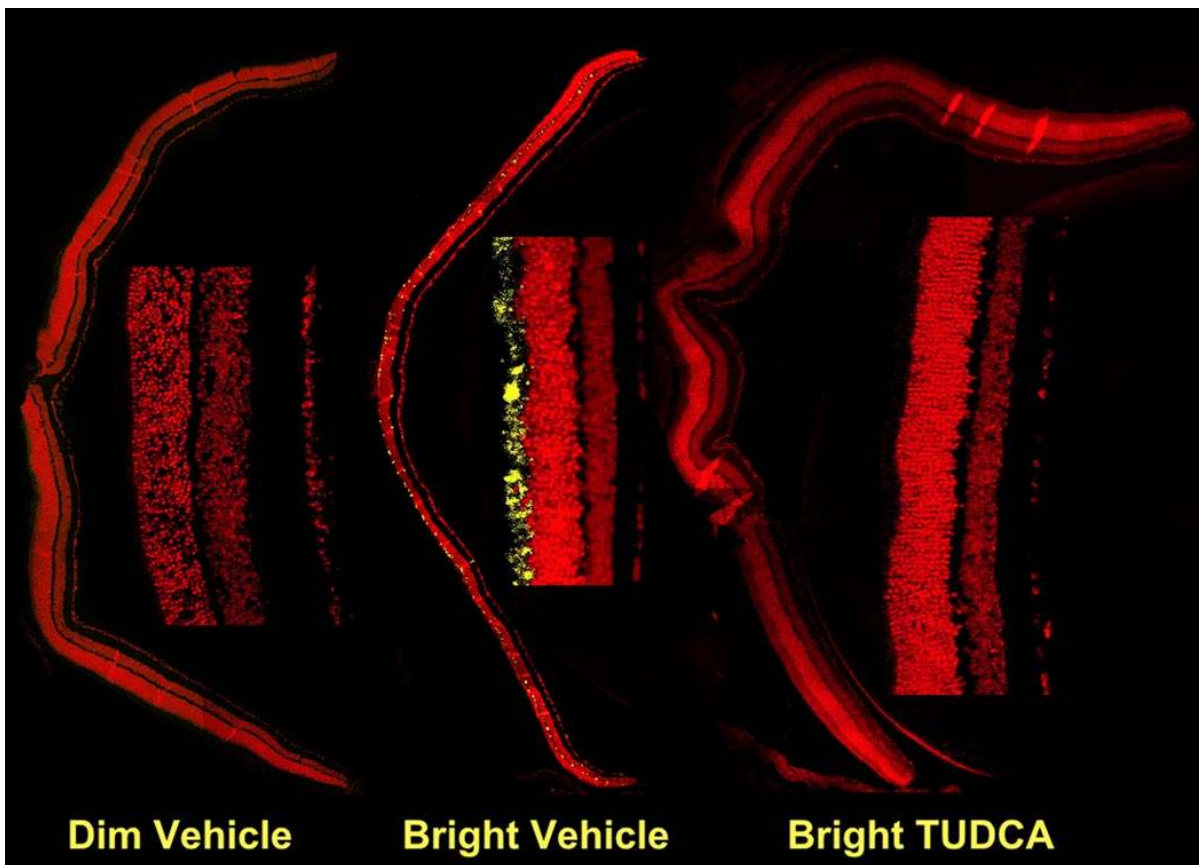
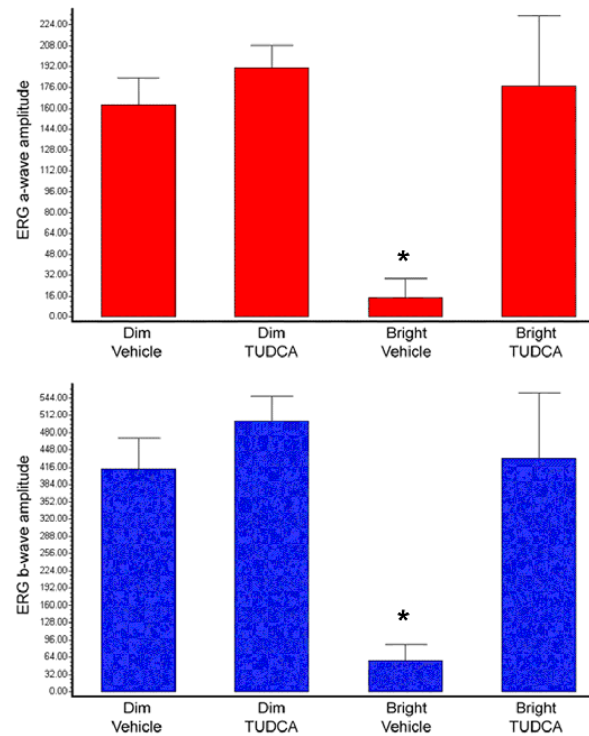


Figure 5. Effect of TUDCA on LIRD mouse retina caspase-3 activation. Confocal micrographs of paraffin-embedded mouse retina sections assayed for immunoreactivity to activated caspase-3 following vehicle or TUDCA injections and exposure to dim or bright light. There was significantly more immunoreactivity (yellow signal) in bright-light exposed vehicle-treated sections than in TUDCA-treated sections (3.2 ± 1.5 versus 0.25 ± 0.16 mean pixel luminosity per section; $p=0.0180$, $t=2.15$, $df=12$).

$F_{(9,369)}=10.04$, $p<0.0001$ for a-wave comparison and $F_{(9,369)}=1.93$, $p=0.047$ for b-wave comparison).

TUDCA treatment preserved photoreceptor number and morphology (Figure 7, Figure 8, Figure 9, and Figure 10). The number of photoreceptor nuclei in the outer nuclear layer (ONL) was significantly greater with TUDCA treatment compared to vehicle treatment (Figure 7; 522 ± 45 versus 355 ± 43 ONL nuclei per 400 μm -wide retinal section; $p=0.0077$). Combined inner segment (IS) and outer segment (OS) length was markedly greater in mice treated with TUDCA compared to vehicle (14.8 ± 1.14 versus 8.12 ± 2.03 μm ; $p=0.0222$), with no change in thickness of inner nuclear layer (INL) or ganglion cell layer (GCL; Figure 7, Figure 8, and Figure 9).

TUDCA injections suppressed apoptosis in *rd10* mice. By P18, about 20% of photoreceptor cell nuclei (but no other cell type) were TUNEL-positive in retinas of vehicle-treated mice (Figure 8 and Figure 9). Conversely, TUDCA-treated retinas showed almost no TUNEL signal (Figure 8 and Figure 9). Significantly more fluorescence was measured in retina sections from vehicle-treated mice than from TUDCA-treated mice (1.21 ± 0.42 , $n=5$ versus 0.09 ± 0.19 , $n=6$ mean pixel luminosity per section; $p=0.0180$). Similarly, retina sections from TUDCA-injected mice exhibited much less immunoreactivity for activated caspase-3 (mean pixel luminosity per whole retina section: 0.09 ± 0.19 , $n=6$ versus 1.21 ± 0.42 , $n=5$; $p=0.0180$ by Student's t-test; Figure 10).

DISCUSSION

TUDCA was readily delivered into mice by subcutaneous injection. Treatment resulted in high levels in the brain (a representative neural tissue) as previously found [8,13,14].

Treatment of LIRD mice resulted in profound inhibition of apoptosis and prevention of the retinal degeneration and ERG amplitude diminution normally seen with the toxic levels of light used here and in other studies (e.g., [7]). The *rd10* genetic model of retinal degeneration perhaps demonstrates a more clinically relevant situation. In *rd10* mice, TUDCA treatment prevented apoptosis and greatly diminished the morphological and functional deficit normally seen in these animals at P18 [4,5], suggesting that TUDCA might be useful for slowing the progression of retinal degeneration in human hereditary retinal disease involving apoptosis.

The data suggest that TUDCA treatment preserved retinal function and morphology, likely by inhibiting caspase-mediated photoreceptor apoptosis. To our knowledge, this is the first controlled, experimental proof of the ophthalmic efficacy of a bear bile constituent, and critically, it was achieved in tests of both environmental and genetic models of retinal degeneration. Though the benefits and mechanism of action of TUDCA have not been examined previously by vision scientists and clinicians, TUDCA and ursodeoxycholic acid (UDCA), the unconjugated form of TUDCA, have been shown to reduce endoplasmic reticulum stress and inflammatory responses in models of diabetes [15] and liver disease [16] and to be cytoprotective and anti-apoptotic in animal models of neurodegeneration, including Huntington disease [13], Parkinson disease [14], and stroke [8]. Similar to these dis-

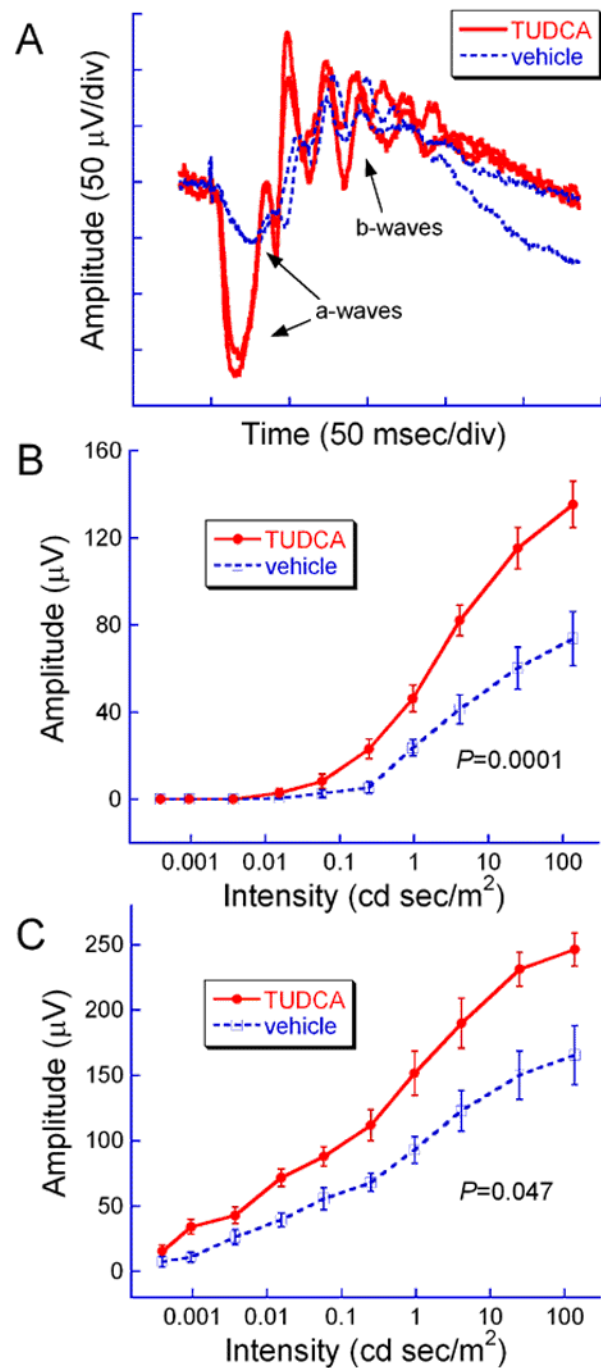


Figure 6. Effect of TUDCA on *rd10* mouse retinal function. **A**: Representative ERG traces from two mice showing large a-waves for TUDCA-treated mice compared to vehicle-treated mice. **B** and **C**: Intensity response functions for dark-adapted a-wave (**B**) and b-wave (**C**) amplitudes of *rd10* mice. TUDCA treatment ($n=11$; red) resulted in significantly greater amplitudes compared to vehicle treatment ($n=12$; blue) as tested by repeated measures ANOVA: $F_{(9,369)}=10.04$, $p<0.0001$ for a-wave comparison (**B**) and $F_{(9,369)}=1.93$, $p=0.047$ for b-wave comparison (**C**), indicating preservation of photoreceptor function. Values are mean \pm sem.

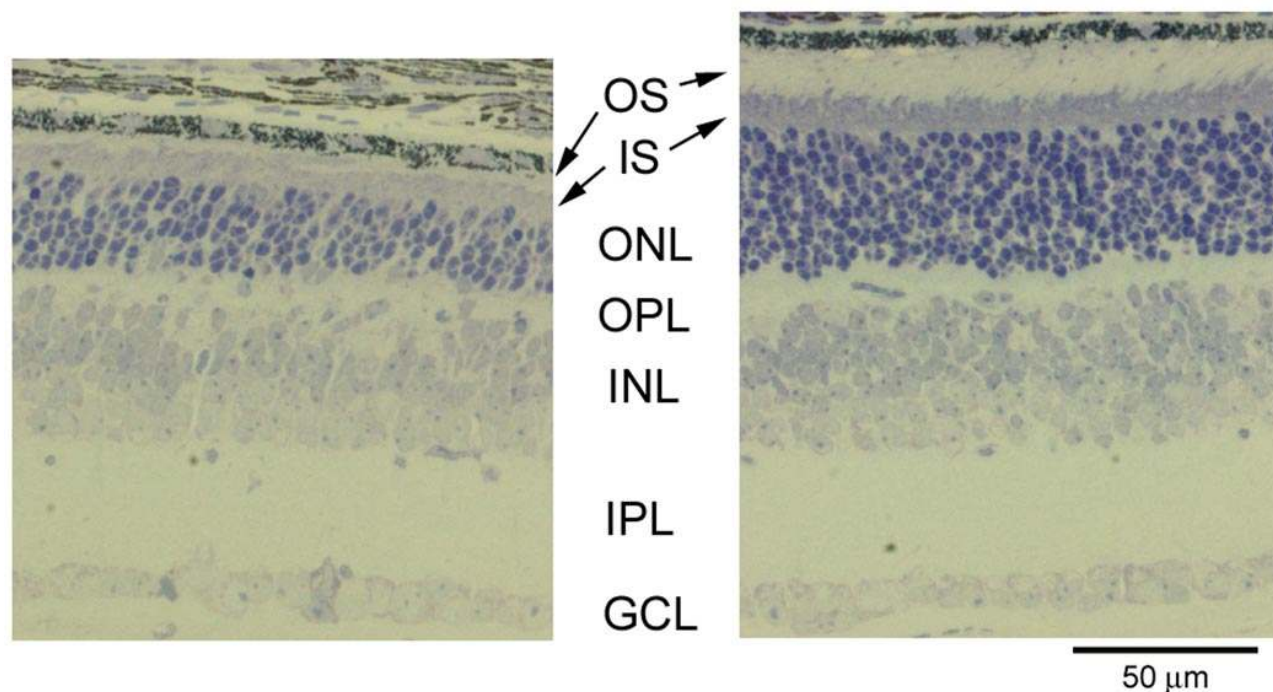


Figure 7. Effect of TUDCA on *rd10* mouse retinal morphology. Representative micrographs stained with toluidine blue showing significant preservation of photoreceptor nuclei in the outer nuclear layer (ONL) in TUDCA treated eyes (right) compared with vehicle treated (left). Counts of photoreceptor nuclei were significantly greater in eyes with TUDCA treatment (right; n=7) compared to vehicle treatment (left; n=9; 522 ± 45 versus 355 ± 43 ONL nuclei per 400 μm -wide retinal section; $p=0.0077$). Combined inner segment (IS) and outer segment (OS) length was similarly preserved (14.8 ± 1.14 versus 8.12 ± 2.03 μm ; $p=0.0222$), with no change in thickness of inner nuclear layer (INL) or ganglion cell layer (GCL).

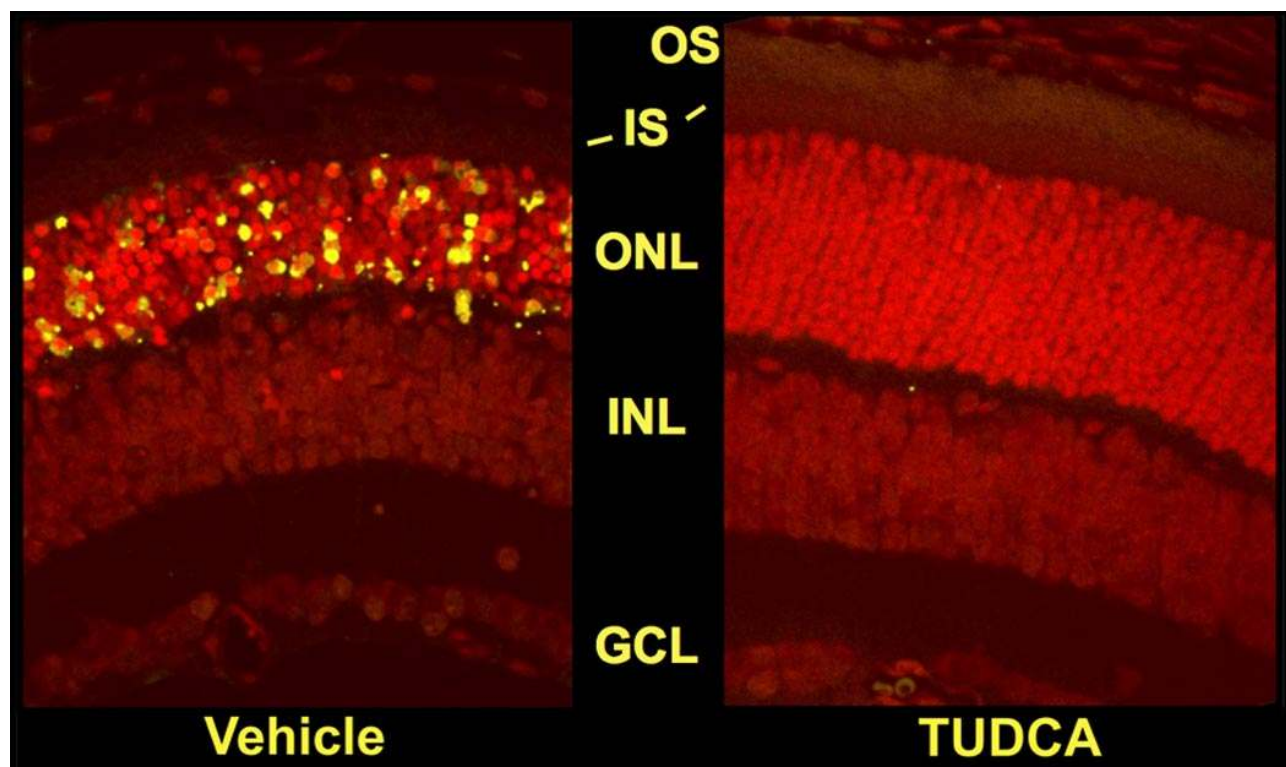


Figure 8. Effect of TUDCA on *rd10* mouse retinal morphology and TUNEL. Confocal micrographs of paraffin-embedded *rd10* mouse retina sections assayed for apoptosis by TUNEL. TUNEL-positive cells (yellow signal) were abundant in vehicle-treated sections, but rare in TUDCA-treated sections ($19.4 \pm 2.24\%$, n=9 versus $0.430 \pm 0.117\%$, n=7; $p < 0.0001$).

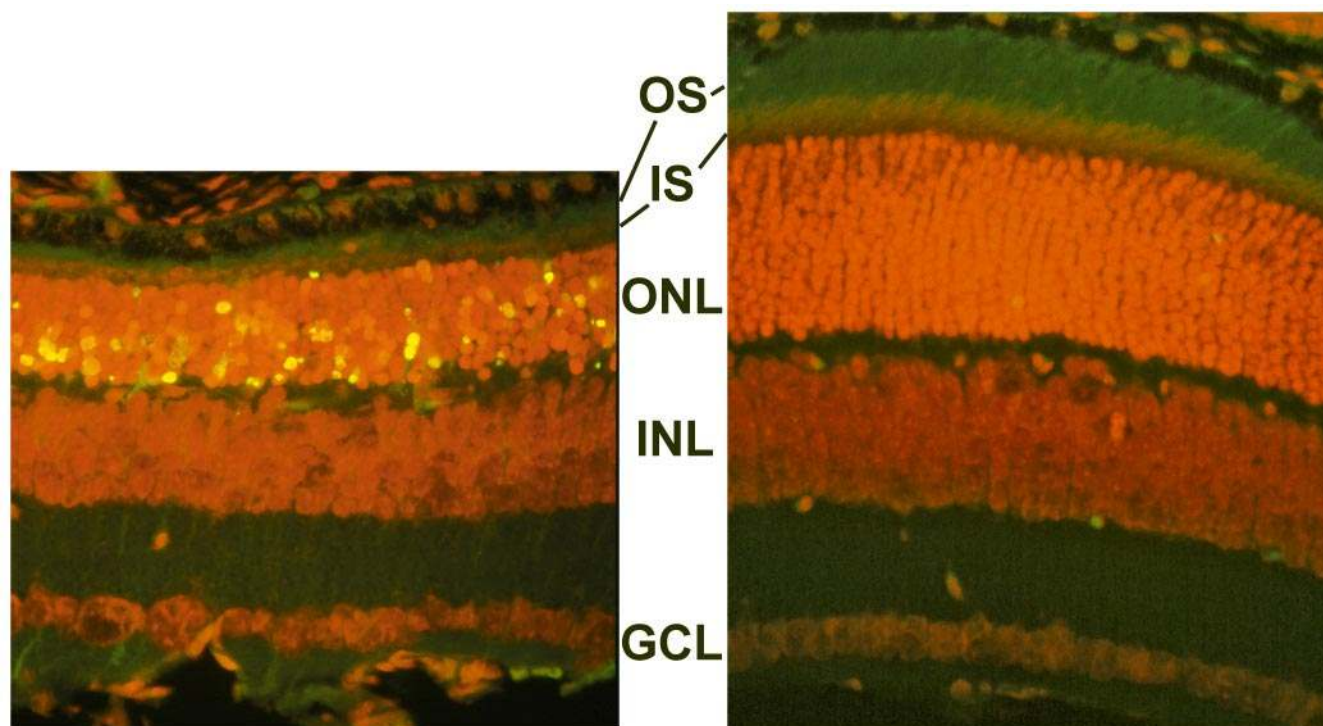


Figure 9. Effect of TUDCA on *rd10* mouse retinal morphology and TUNEL: Further observation. Fluorescence microscopy using a B-2A longpass emission fluorescence filter allows further observation of the preservation of photoreceptor inner segments (IS) and outer segments (OS; the light-capturing structure of the cell) present in TUDCA-treated (right) versus vehicle-treated retina sections (left). Similar to confocal imagery (Figure 8), TUNEL-positive nuclei (green/yellow signal) are seen to be abundant in vehicle-treated sections, but rare in TUDCA-treated sections. TUDCA treatment provided significant preservation of photoreceptor nuclei number in the outer nuclear layer (ONL). Treatment had no discernable effect on the inner nuclear layer (INL) or ganglion cell layer (GCL).

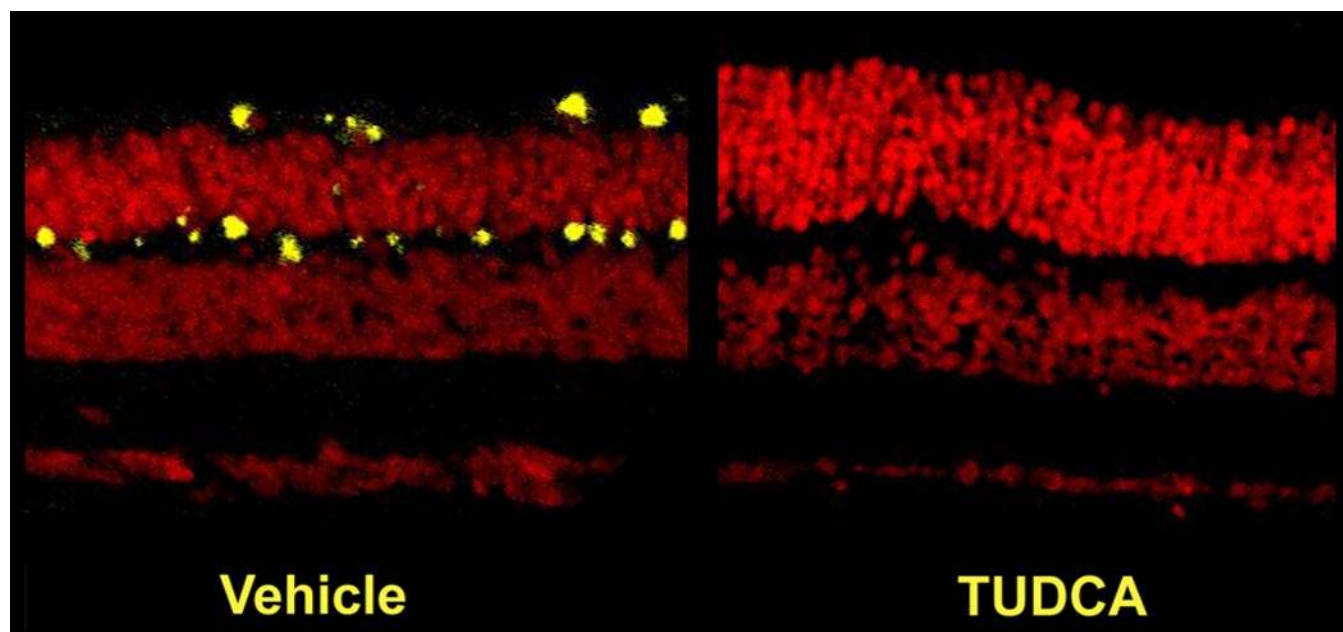


Figure 10. Effect of TUDCA on *rd10* mouse retinal morphology and activated caspase-3 immunoreactivity. Confocal micrographs of paraffin-embedded *rd10* mouse retina sections assayed for immunoreactivity to activated caspase-3. There was significantly more immunoreactivity (yellow signal) in vehicle-treated sections than in TUDCA-treated sections (1.21 ± 0.42 , $n=5$ versus 0.09 ± 0.19 , $n=6$ mean pixel luminosity per section; $p=0.0180$).

eases, apoptosis is central to the etiologies of several forms of human blindness such as age-related macular degeneration [17,18], retinitis pigmentosa [6], and glaucoma [6,19]. These diseases affect more than 100 million people worldwide, a number that will increase as the population ages. The potential relevance of our results to world health is further underscored when it is considered that synthetic hydrophilic bile acids are inexpensive, well tolerated at high doses in humans, and are already FDA approved for treatment of human liver disease [2,16].

ACKNOWLEDGEMENTS

Supported by Foundation Fighting Blindness, Research to Prevent Blindness, Knights Templar Education Foundation, the Biomedical Research Service, Department of Veterans Affairs, and NIH grants R01 EY014026, P30 EY06360, R01 EY012514, P30 AT000609, R01 EY016470, R01 EY07758, and R24 EY017045. The authors gratefully acknowledge input from Animals Asia Foundation and TRAFFIC East Asia on the use of bear bile in Traditional Medicine and the availability of synthetic alternatives. No bears were harmed and no bear products were used in any facet of these studies. Yu Yang, M.D. (Emory University) aided us by interpreting ancient and modern Chinese texts. Some of the data presented here were presented in abstract form at annual meetings of the Association for Research in Vision and Ophthalmology [20,21].

REFERENCES

- Cidian, ZYD, editor. Dictionary of Traditional Chinese Medicine, Vol. 2. Shanghai, China: Shanghai Science and Technology Press; 2004.
- Williamson DF, Phipps MJ. editors. Proceedings in the Third Annual Symposium on the Trade in Bear Parts 1999. Hong Kong, China: TRAFFIC East Asia; 2001.
- Sola S, Garshelis DL, Amaral JD, Noyce KV, Coy PL, Steer CJ, Iazzo PA, Rodrigues CM. Plasma levels of ursodeoxycholic acid in black bears, *Ursus americanus*: seasonal changes. *Comp Biochem Physiol C Toxicol Pharmacol* 2006; 143:204-8.
- Chang B, Hawes NL, Hurd RE, Davisson MT, Nusinowitz S, Heckenlively JR. Retinal degeneration mutants in the mouse. *Vision Res* 2002; 42:517-25.
- Chang B, Hawes NL, Pardue MT, Rengarajan K, German AM, Hurd RE, Davisson MT, Nusinowitz S, Boyd AP, Sidney SS, Stewart RE, Chaudhury RC, Nickerson JM, Heckenlively JR, Boatright JH. Two mouse retinal degenerations caused by missense mutations in the beta-subunit of rod cGMP phosphodiesterase gene. *Vision Res*. In press 2007.
- Reme CE, Grimm C, Hafezi F, Marti A, Wenzel A. Apoptotic cell death in retinal degenerations. *Prog Retin Eye Res* 1998; 17:443-64.
- Chen L, Dentchev T, Wong R, Hahn P, Wen R, Bennett J, Dunaief JL. Increased expression of ceruloplasmin in the retina following photic injury. *Mol Vis* 2003; 9:151-8.
- Rodrigues CM, Sola S, Nan Z, Castro RE, Ribeiro PS, Low WC, Steer CJ. Tauroursodeoxycholic acid reduces apoptosis and protects against neurological injury after acute hemorrhagic stroke in rats. *Proc Natl Acad Sci U S A* 2003; 100:6087-92.
- Setchell KD, Rodrigues CM, Clerici C, Solinas A, Morelli A, Gartung C, Boyer J. Bile acid concentrations in human and rat liver tissue and in hepatocyte nuclei. *Gastroenterology* 1997; 112:226-35.
- Jablonski MM, Dalke C, Wang X, Lu L, Manly KF, Pretsch W, Favor J, Pardue MT, Rinchik EM, Williams RW, Goldowitz D, Graw J. An ENU-induced mutation in *Rslh* causes disruption of retinal structure and function. *Mol Vis* 2005; 11:569-81.
- Pardue MT, McCall MA, LaVail MM, Gregg RG, Peachey NS. A naturally occurring mouse model of X-linked congenital stationary night blindness. *Invest Ophthalmol Vis Sci* 1998; 39:2443-9.
- Pardue MT, Phillips MJ, Yin H, Sippy BD, Webb-Wood S, Chow AY, Ball SL. Neuroprotective effect of subretinal implants in the RCS rat. *Invest Ophthalmol Vis Sci* 2005; 46:674-82.
- Keene CD, Rodrigues CM, Eich T, Chhabra MS, Steer CJ, Low WC. Tauroursodeoxycholic acid, a bile acid, is neuroprotective in a transgenic animal model of Huntington's disease. *Proc Natl Acad Sci U S A* 2002; 99:10671-6.
- Duan WM, Rodrigues CM, Zhao LR, Steer CJ, Low WC, Rodrigues CM. Tauroursodeoxycholic acid improves the survival and function of nigral transplants in a rat model of Parkinson's disease. *Cell Transplant* 2002; 11:195-205. Erratum in: *Cell Transplant*. 2002; 11:619.
- Ozcan U, Yilmaz E, Ozcan L, Furuhashi M, Vaillancourt E, Smith RO, Gorgun CZ, Hotamisligil GS. Chemical chaperones reduce ER stress and restore glucose homeostasis in a mouse model of type 2 diabetes. *Science* 2006; 313:1137-40.
- Beuers U, Spengler U, Kruis W, Aydemir U, Wiebecke B, Heldwein W, Weinzierl M, Pape GR, Sauerbruch T, Paumgartner G. Ursodeoxycholic acid for treatment of primary sclerosing cholangitis: a placebo-controlled trial. *Hepatology* 1992; 16:707-14.
- Nordgaard CL, Berg KM, Kappahn RJ, Reilly C, Feng X, Olsen TW, Ferrington DA. Proteomics of the retinal pigment epithelium reveals altered protein expression at progressive stages of age-related macular degeneration. *Invest Ophthalmol Vis Sci* 2006; 47:815-22.
- Adler R, Curcio C, Hicks D, Price D, Wong F. Cell death in age-related macular degeneration. *Mol Vis* 1999; 5:31.
- Zalewska R, Reszec J, Mariak Z, Sulkowski S. [The expression of Bcl-2, Bcl-xl, Bak and Bax proteins in axons of the optic nerve in closed-angle glaucoma]. *Klin Oczna* 2004; 106:155-7.
- Boatright JH, Boyd AP, Sidney SS, Minear SC, Stewart RE, Chaudhury R, Ciavatta VT. Effect of Tauroursodeoxycholic Acid on Light-Induced Retinal Degeneration. *ARVO Annual Meeting*; 2006 April 30-May 4; Fort Lauderdale (FL).
- Boatright JH, Moring AG, McElroy CE, Do VT, Phillips MJ, Nickerson JM, Pardue MT. Effect of tauroursodeoxycholic acid on retinal degeneration in rd10 mice. *ARVO Annual Meeting*; 2004 April 25-29; Fort Lauderdale (FL).

The print version of this article was created on 30 Dec 2006. This reflects all typographical corrections and errata to the article through that date. Details of any changes may be found in the online version of the article. α